20th Australasian Fluid Mechanics Conference
Perth, Australia
5-8 December 2016

Preliminary Investigation of Sound Generation in Scramjets

N. Gibbons[1], V. Wheatley[1] and C. Doolan[2]

[1]School of Mechanical and Mining Engineering
University of Queensland, St. Lucia QLD 4072, Australia

[2]School of Mechanical and Manufacturing Engineering
University of New South Wales, Sydney NSW 2052, Australia

Abstract

Aeroacoustic noise generation in scramjet engines is investigated, by analyzing Hybrid RANS/LES simulations of a simplified engine-like geometry. Pressure data collected over a statistically long period are analyzed in the frequency domain, revealing a number of modes in the 100-200 kHz range which contribute significantly to the overall fluctuating noise level. Visualization of fluctuating quantities also shows a sequence of waves being generated by the fuel injection process which seem to propagate acoustically into the surrounding flow. This analysis shows that the LES methodology employed is capable of resolving the low-amplitude waves found in acoustics problems, and justifies future research to evaluate the accuracy the technique against experimental and theoretical results.

Introduction

Commercial air transport in the twenty-first century is safe, routine, and inexpensive, linking the citizens of the world across vast distances and national borders. In contrast, modern space flight remains a difficult undertaking, fraught with risk and technical complexity that limits the extent of our orbital resources and the scientific exploration of the final frontier. Development of reusable hypersonic aircraft is part of a strategy to improve this problem by making flexible new launch systems that are not destroyed with each mission, but any such aircraft must survive exposure to extreme flight conditions and return safely to fly again and again.

A significant hazard of high speed flow is aeroacoustic vibration generated by the fluid itself, which affects the fatigue life of the structure and the safe operating limits of the onboard electronics. This is a critical issue identified in [1], but at present very little is known about how to predict flow noise at hypersonic speeds or how to design countermeasures to dampen sound generation sources inside the flow. To begin with, we must determine whether the numerical tools available have sufficient fidelity to capture low amplitude sound waves generated in the engine. This is a simple question that will inform future testing to actually validate the numerical predictions against experiments and theoretical models.

Numerical Method

Simulations are performed using UnStructured 3D (US3D): A hybrid structured/unstructured compressible fluid dynamics solver for complex geometries [2], developed at the University of Minnesota. US3D is used to study hypersonic flows that require implicit timestepping to due viscous boundary layers, turbulence modelling appropriate for separated shear flow, and non-equilibrium chemistry models for fuel and air reactions. In this work we simulate flow through an idealized model scramjet suitable for fundamental combustion experiments, shown in figure 1.

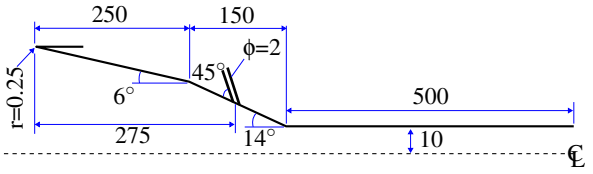

Figure 1: Geometry of model scramjet, symmetric below the centreline except with no injector. Depth is planar periodic with a span of 40mm. All dimensions are in mm.

Hypersonic air enters the simulation domain from the left and is compressed by two intake ramps to reach autoignition conditions (above $\approx 50kPa$ and $1600K$). Hydrogen fuel is then injected on the second intake ramp and combustion occurs in a long constant area section downstream. The simulation is planar periodic with a depth of $40mm$, and is symmetric about the centerline, except for the fuel injector which is only on the upper surface. A supersonic inflow boundary condition is used, designed to result in flight representative conditions in the combustor (see table 1).

Boundary Conditions		
Inflow	ρ	0.01044 $kg.m^{-3}$
	T	213.0 K
	p	640.7 Pa
	v	3037.0 $m.s^{-1}$
	M	10.36
	Y_{O_2}	0.233
	Y_{N_2}	0.767
Fuel Jet	p_t	1.468 MPa
	T_t	300 K
	$\dot{m}$	0.0108 $kg.s^{-1}$
	v	1145 $m.s^{-1}$
	Y_{H_2}	1.00
Wall	T	300 K

Table 1: Inflow Conditions for scramjet model with periodic sidewalls.

Chemical reactions are handled using the non-equilibrium hydrogen oxidation scheme of [3] and turbulence is modelled using the IDDES Hybrid RANS/LES method described in [4]. Thermal equilibrium gas modelling is used, employing the thermodynamic tables published by [5]. A 6th order accurate gradient reconstruction method is used to compute the inviscid fluxes, blended with the dissipative part of the modified Steger-Warming method near discontinuities to capture shockwaves. Time advancement is performed with 2nd order accurate implicit Euler integration, using a blending function to transition to a first order time accuracy near solid walls to preserve numerical stability in the boundary layer.

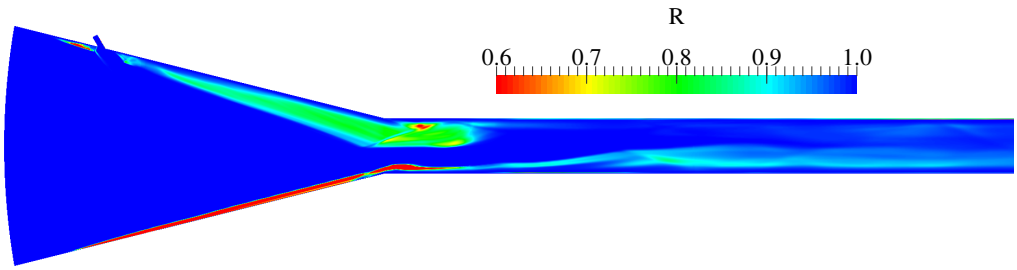

Figure 2: Time average of the fraction of modelled turbulent kinetic energy in the total TKE.

Simulation Quality

Large Eddy Simulation uses high resolution grids and terascale supercomputing to resolve actual turbulent fluctuations as part of the simulation. Since the smallest scales of the turbulence are still missing, their influence is accounted for by using a subgrid model, in our case the Spalart-Allmaras based IDDES framework, to remove energy from the large scales at approximately the correct rate. Proper grid refinement is critical to the technique, but also difficult to check since the solutions are unsteady and subgrid quantities can only ever be estimated. The final grid chosen by our grid refinement study uses fully structured hexahedral cells constrained to be as cubic as possible, with side lengths as given below:

Final Grid Details	
Total Cell Count	37,817,312
Inlet Wall Cell Height	$1\mu m$
Combustor Wall Cell Height	$0.5\mu m$
Injector Cell Size	$0.04mm$
Jet Cell Size	$0.1mm$
Jet Wake Cell Size	$0.25mm$
Combustor Entrance Cell Size	$0.2mm$
Combustor Core Cell Size	$0.4mm$

To evaluate the level of discretisation used, we have used the method of [6] to estimate the subgrid turbulent kinetic energy (TKE) and compare it in magnitude to the resolved TKE present in the flow. The resolved TKE is computed from the fluctuating velocities $u_i' = u_i - \overline{u_i}$. Using index summation over the velocity vector u_i, Δ as the filter width, c_v^k a constant equal to 0.07, and the overline operator to denote a time average, the subgrid and resolved TKE are:

$$k_{sgs} = \frac{\nu_t^2}{(c_v^k \Delta)^2} \quad k_r = \frac{1}{2} u_i' u_i' \tag{1}$$

According to a classical definition of a well resolved LES, there should be around 80% of the total TKE present in the resolved scales. Figure 2 shows $R = \overline{k_r/(k_r + k_{sgs})}$ on the symmetry plane, where green values indicate the subgrid model is active to an acceptable degree and red indicates trouble spots where the modelled TKE is comparatively higher. Red areas in front of the injector and on the bottom wall occur because flow here is modelled with RANS, as per the intended DES mechanics, and there is no resolved motion. Because of this, the R criterion is misleading in these areas. The other red spot, at the upper combustor entrance, is caused by a separation in this region that appears to be unusually laminar and steady. In this area we believe the subgrid TKE is being over estimated by our approximation method, and the flow is probably well resolved enough for the present purposes. More investigation into this area may be required.

Time discretisation is dominated by the need to resolve the signal propagation time in the cubic cells near the front edge of the injector, which need an effective CFL number of around one to ensure time accuracy. A constant timestep of $7ns$ is used to enforce this (see figure 3).

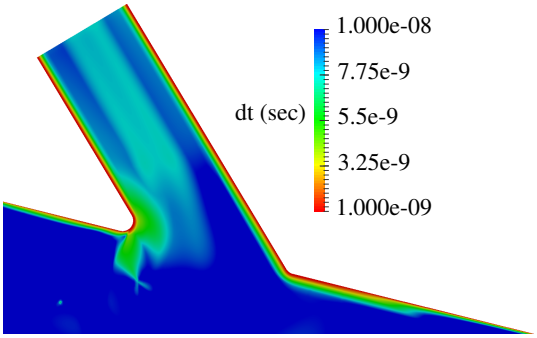

Figure 3: Estimated maximum timestep for explicit stability based on CFL criteria.

Boundary layers are resolved by clustering the cells into the wall so that the first cell's height is $y^+ < 1$ in wall units. This ensures that the RANS model that is active below the log layer has sufficient cells to perform accurately near the wall. Figure 4 shows the nondimensional first cell height for the upper and lower walls, averaged over the spanwise direction. Note that there is a peak in the upper surface due to the injector having larger cell sizes than the surrounding wall, but the maximum y^+ in the injector is still around one.

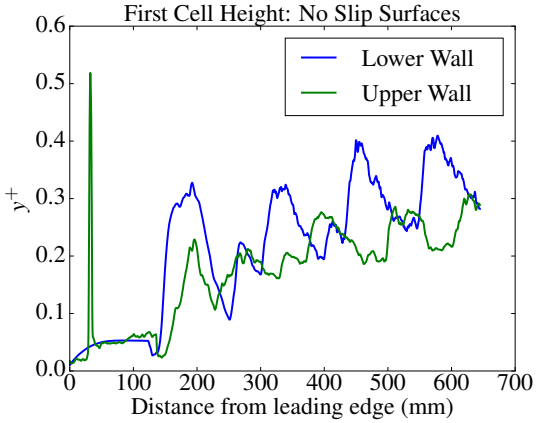

Figure 4: Spanwise average first cell height along the downstream direction in nondimensional wall units.

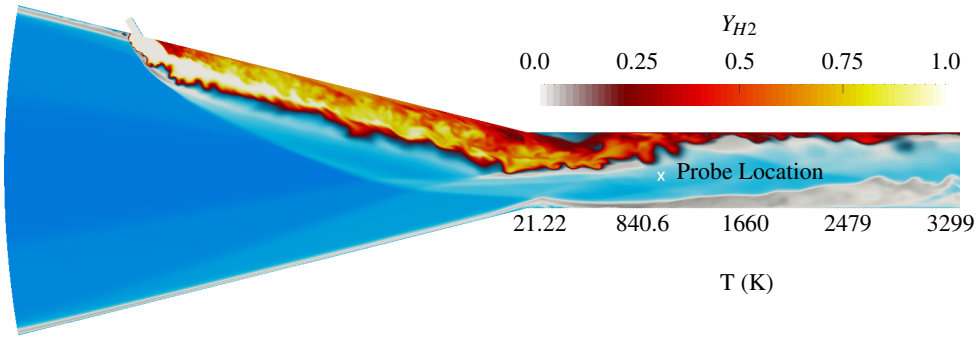

Figure 5: LES simulated flow field showing hydrogen mass fraction and temperature fields. Probe point is marked with an x.

Unsteady Pressure Loading

The simulation results contain actual turbulent fluctuations that emerge from the Navier-Stokes equations in physically unstable phenomena like shear layers, shock/boundary layer interactions and baroclinic interfaces where the pressure and density gradients are misaligned. These create pressure fluctuations throughout the domain that are propagated by convection and conventional turbulence, but also via compressible waves that travel faster than the surrounding fluid velocity. In the limit of very weak disturbances these become sound waves, which can travel great distances by acoustic propagation away from their parent flowfields.

To investigate the unsteady loading in the engine, we have placed a virtual probe into the combustor entrance (see figure 5) and recorded the filtered pressure at one cell over a large number of timesteps. The fluctuations are produced by both acoustic and convection mechanisms, combining them into a simple measurement of the unsteady pressure load produced inside the engine from purely fluid mechanical sources.

Figure 6 shows the pressure fluctuations at the probe point, computed by subtracting the average pressure over the entire time period from the signal. The flow-through time of the engine, defined as the length from the injector to the outflow divided by the freestream velocity, is around 200 μs; so the data collection period should be long enough to capture any long periodic cycles present in the turbulence.

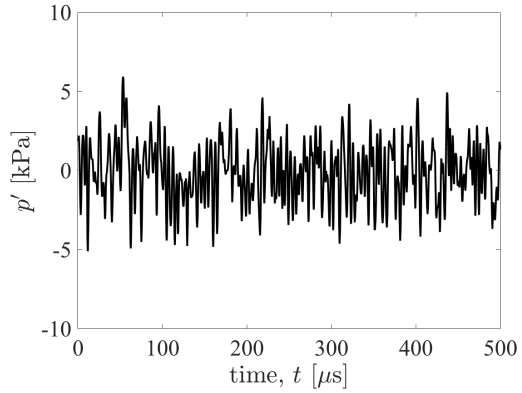

Figure 6: Fluctuating pressure $p' = p - \overline{p}$ at the probe location.

The power-spectral density of the trace is depicted in figure 7, showing some specific frequencies in the 100-200 kHz range make significant contributions to the overall pressure load at this point.

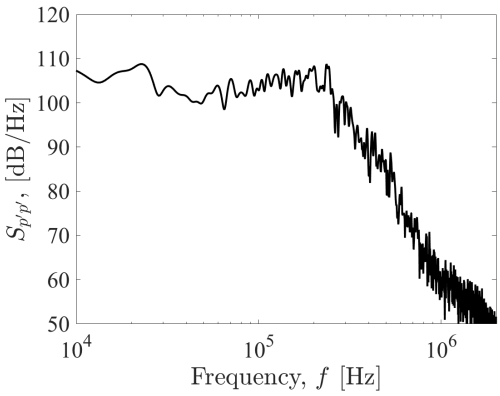

Figure 7: Power spectral density of pressure history from figure 6.

These results show that there is an interesting band of frequencies responsible for the largest contribution to the unsteady pressure load, which could be compared to frequency measurements from other places to isolate which source of vibration is responsible for the largest fraction of the computed loading. The dominant frequencies could be generated by the shedding cycle of the fuel jet, which tends to produce coherent Kelvin-Helmholtz vorticies at a frequency distribution characterized by a dominant mode. Shock/boundary layer interactions also occur in any hypersonic vehicle, producing oscillations at significantly lower frequencies than the turbulence in the underlying boundary layer [7]. Both of these are sources of unsteady load in a scramjet engine that may be good targets for noise mitigation measures.

Wave Visualization

Elsewhere in the simulation we can try to visualize waves produced by the injection process. From the time average and instantaneous temperature fields, the fluctuating temperatures may be computed using $T' = T - \overline{T}$. Figure 8 depicts the magnitude of the gradient of this quantity at a late time when the unsteady flow is statistically stationary.

Emanating from the injector is a plume of turbulent hydrogen fuel, visible as the complex turbulent region of high $|\nabla T'|$. Between the plume and the bow shock is a section of relatively clean flow overlayed with some low amplitude fluctuations, appearing as a series of striations or filaments, stretching away from the fuel plume and appearing to reflect of the jet's pri-

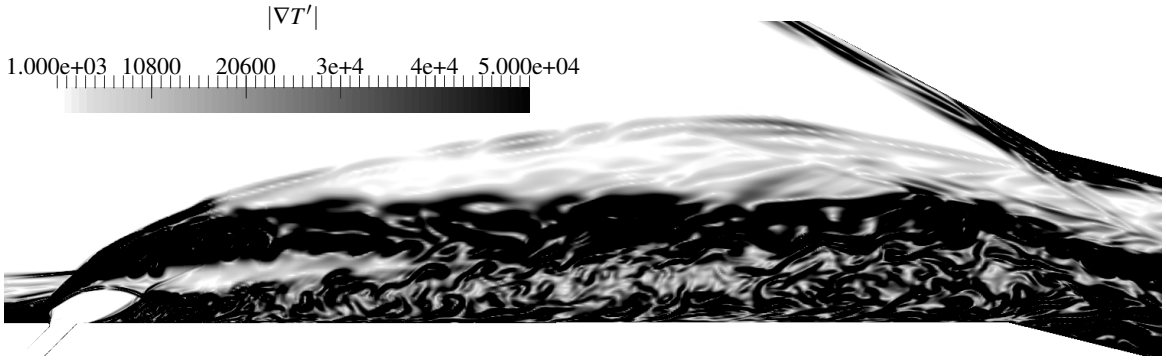

Figure 8: Magnitude of the Temperature Fluctuation gradients, $|\nabla T'|$ where $T' = T - \overline{T}$.

mary shockwave. We hypothesize that these filaments are sound waves, transported by wavelike mechanisms away from the turbulent jet interface and into the comparatively steady flow. To investigate this, consider figure 9, showing the mach angles in this region overlayed on the $|\nabla T'|$ field. The mach angle is the angle at which an acoustic disturbance propagates in a supersonic flow, given by:

$$\mu = tan^{-1}\left(\frac{v}{u}\right) \pm tan^{-1}\left(\frac{a}{\sqrt{u^2+v^2}}\right) \qquad (2)$$

Where a is the sound speed. Visual inspection of this figure suggests that the filaments in this region seem to line up reasonably closely with the mach angles, noting that the negative sign in equation 2 allows the waves to travel downward as well, symmetric to the flow velocity vector.

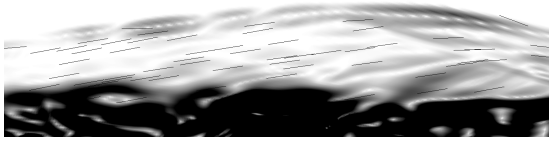

Figure 9: Mach angle glyphs overlayed on figure 8.

Conclusions

In this paper we have investigated the suitability of an LES compressible flow code for simulating flow-induced noise in scramjet engines. We have considered a hybrid RANS/LES calculation of a turbulent reacting flow in a model scramjet, of a type suitable for a fundamental combustion experiment but with periodic sidewalls. The simulations contain a number of low-amplitude waves present in regions where the unsteady jet plume does not reach, generated by the turbulent flow driving disturbances into the surrounding flow. This conclusion is supported by an analysis of the theoretical angle of propagation for an acoustic disturbance that appears to match the numerical results quite well. The power spectral density of a single point in the combustor also showed the signatures of flow induced pressure fluctuations at several distinct frequencies that contribute significantly to the overall fluctuating load. Whether the overall predictions and the computed spectrum are accurate must be determined by future comparison to experimental data, but in the mean time these results suggest that further aeroacoustic research using LES will be a worthwhile enterprise.

Acknowledgements

The authors would like to thank Professor Graham Candler's research group for providing the research CFD code used. Supercomputer time was provided by the National Computational Infrastructure (NCI) at the ANU and by the Pawsey Supercomputing Centre in WA, supported by an award under the NCI Merit Allocation Scheme and funding from the Australian Government.

V. Wheatley was supported an Australian Research Council Discovery Early Career Researcher Award (project number DE120102942).

References

[1] T. G. Eason, S. M. Spottswood, R. Chona, and R. Penmetsa, "A structures perspective on the challenges associated with analyzing a reusable hypersonic platform," in *54th AIAA/ASME/ASCE/AHS/ASC Structures, Structural Dynamics and Materials Conference*, no. 2013-1747, (Boston, Massachusetts), 2013.

[2] I. Nompelis, T. W. Drayna, and G. V. Candler, "Development of a hybrid unstructured implicit solver for the simulation of reacting flows over complex geometries," in *34th AIAA Fluid Dynamics Conference*, (Portland, Oregon), 28th June-1st July 2004.

[3] C. J. Jachimowski, "An analysis of combustion studies in shock expansion tunnels," Tech. Rep. NASA TP-3224, National Aeronautics and Space Administration, July 1992.

[4] M. Shur, P. Spalart, M. Strelets, and A. Travin, "A hybrid rans-les approach with delayed-des and wallmodelled les capabilities," *International Journal of Heat and Fluid Flow*, vol. 29, pp. 1638–1649, 2008.

[5] B. J. McBride, M. J. Zehe, and S. Gordon, "Nasa glenn coefficients for calculating thermodynamic properties of individual species," Tech. Rep. 211556, National Aeronautics and Space Agency, 2002.

[6] R. M. Gehre, *The Flow Physics of Inlet-Fueled, Low-Compression Scramjets*. PhD thesis, The University of Queensland, School of Mechanical and Mining Engineering, 2014.

[7] D. V. Gaitonde, "Progress in aerospace sciences," *Progress in Aerospace Sciences*, vol. 72, pp. 80–99, 2015.